Predictive modeling of blast induced ground vibration using RF-PSO-SVM

Paulo Lopes[1]
Hernani Lima[2]

Abstract

In the mining industry, blasting operation is an effective method for rock fragmentation. Blast-induced is one of the most harmful undesirable outcomes produced by blasting operations. When rising to a certain level, it can cause discomfort for humans living in surrounding communities, and damage to civil constructions. Therefore, the prediction and control of ground vibration gain attention in the literature. Peak particle velocity (PPV) is widely used as the indicator of the magnitude of ground vibration. Thus, the main objective of this paper is to establish an accurate and universal tool for PPV prediction. This study implemented a novel non-linear model based on a support vector machine (SVM), particle swarm optimization (PSO) and random forest (RF) (the proposed model is so called RF-PSO-SVM). Multivariate linear regression (MLR) and three popular empirical models are implemented and compared with the proposed model. The dataset utilized in this paper was collected in a mine located in Istanbul. The results indicate that PSO-SVM has a competitive accuracy with the highest R^2 (R-squared value) of 0.7716, least MSE (Mean squared error) of 13.5979 and least MAE (Mean absolute error) of 2.7550. In terms of stability analysis, 10-fold cross-validation was applied. The results reveal that RF-PSO-SVM had the optimal ability of generalization as it had the steadiest prediction variance over different validation groups. The proposed non-linear model presents the feasibility and superiority of blast-induced ground vibration prediction and control.

Keywords

Blast-induced ground vibration; Peak particle velocity; Non-linear regression; Support vector machine; Particle swarm optimization.

[1] Co-founder - Beyond Mining - paulo@beyondmining.tech
[2] Researcher and Professor - UFOP - hernani.lima@ufop.edu.br

Introduction

In the mining industry, blasting is currently the most widely accepted rock fragmentation approach to break the hard rock into appropriate segments to facilitate the following operations and handling. However, about 20–30% of the explosive energy released in blasting is utilized for rock fragments (Dumakor-Dupey et al., 2021), which means the rest of the energy may lead to undesirable outcomes, including air pressure, ground vibration, fly rock, and so on. These undesirable outcomes can threaten the surrounding communities when they reach elevated levels. Ground vibration is one of the main undesirable products of blasting, which arguably cause discomfort to humans living around, damage to constructed buildings close to the mine in the blasting process, affect groundwater, etc (Armaghani et al., 2018; Bisoyi & Pal, 2020). Thus, the prediction of PPV is a valuable research topic.

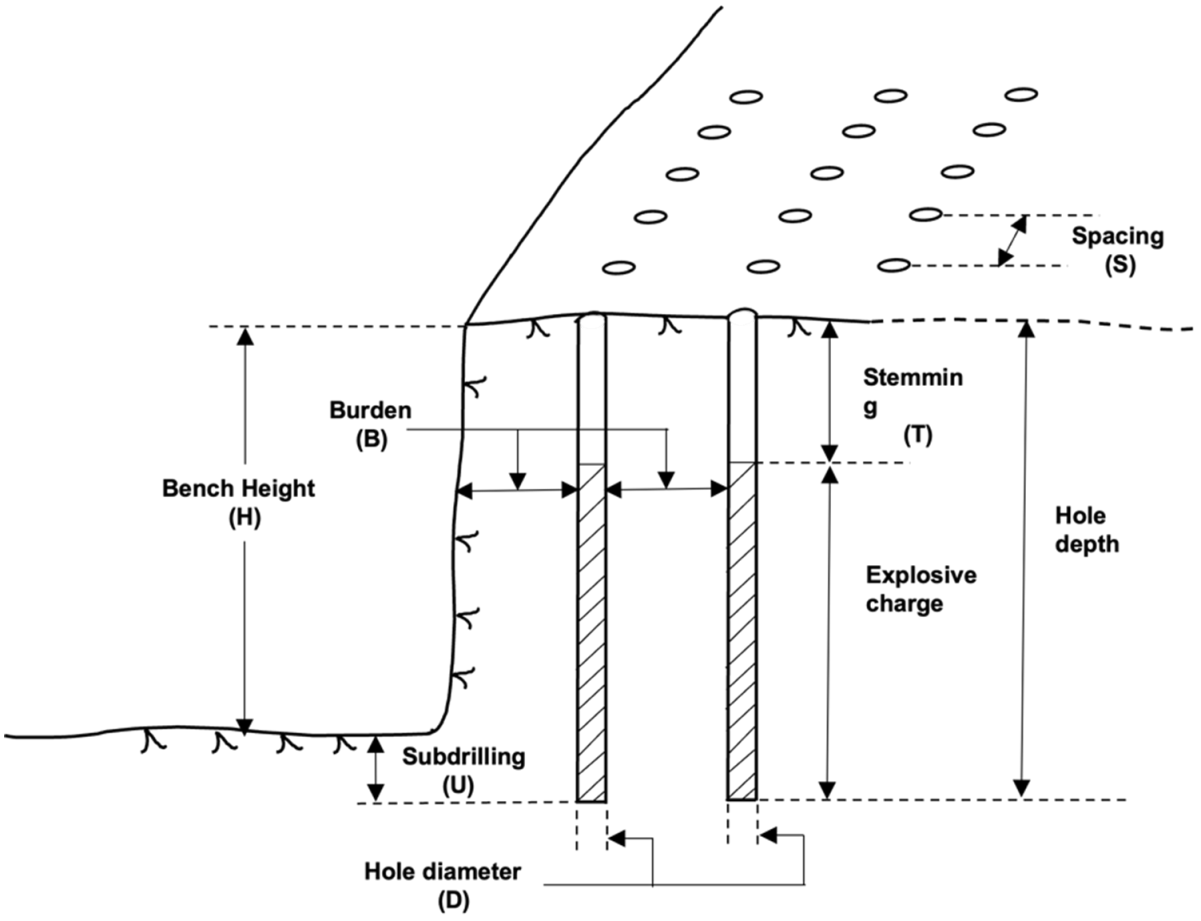

Figure 1 Blast design parameters

Effective parameters

Generally, the parameters affecting blast-induced ground vibration can be categorized into controllable and uncontrollable parameters (Ak et al., 2009; Kabwe et al., 2015). The controllable factors are designed and decided by engineers, including blast design parameters and explosive design parameters. The blast design parameters (or called blast geometries) are the arrangement of the explosive group (illustrated in figure 1), they are bench height, spacing, stemming, blasthole diameter, blasthole depth, burden and subdrilling. The explosive design parameters are power factor and maximum charge per delay. By contrast, the uncontrollable factors are mainly geological constant formations (density, rock strength, rock type, etc,.), which are collected by experiment and field investigation.

Peak particle velocity (PPV) is usually measured to represent the magnitude of ground vibration (Armaghani et al., 2018). It is widely used to show the extent of the damage in the literature, which is positively related to the blast-induced ground strain (Athanasopoulos & Pelekis, 2000; Bisoyi & Pal, 2020; Ghosh & Daemen, 1983). The controllable and uncontrollable factors introduced above can significantly determine the PPV(Amiri et al., 2016; Hasanipanah et al., 2017). The dependency of PPV on these parameters varies a lot (Khandelwal & Singh, 2006; Nateghi, 2011). To provide an excellent prediction, the selection of features is important. In this study, the feature parameters are chosen based on importance computed by a random forest (RF) algorithm.

Empirical models

Many empirical models have been developed based on various parameters.

Among the parameters, it is found that the maximum charge per delay and distance are the most dominant factors for ground vibration prediction (Larson, 1979; E. L. Liu et al., 2011). The empirical models are permanently established following field measurement and experiment trials. However, these two parameters are found not sufficient to predict accurate PPV value due to the complexity of the non-linearity of the relationship (Khandelwal et al., 2009; Singh et al., 2004). Moreover, the empirical models are site-specific due to the heterogeneity of site conditions (Deng et al., n.d.; Kumar et al., n.d.; Kuzu, 2008). The empirical models implemented in this paper are described in section 3.7.2.

Machine learning techniques

The predictors have been enhanced with the development of machine learning (ML) techniques. This section introduces a brief background of two popular ML- based methods (multivariate linear regression and support vector machine).

Multivariate linear regression

Multivariate linear regression (MLR) is an approach to modelling the linear relationship involving multi variables. To utilize the controllable parameters for prediction, MLR has been developed by various researchers (Hudaverdi, 2012; Monjezi et al., 2016; Navarro Torres et al., 2018). In the literature, its performance is limited as the relationship between input parameters and PPV is not linear, which is a challenge of PPV prediction (Gorai et al., 2021; Saadat et al., 2014).

Support vector machine

Another challenge in PPV prediction is the lack of data. The available datasets are in small sample sizes due to the high cost and difficulties of data collection. In this context, Support vector machine (SVM), which has the ability to solve with small samples, was introduced, and developed (Cherkassky et al., n.d.; Flake & Lawrence, 2002). SVM is the basic algorithm in this study.

SVM is an ML method that uses the concept of hyperplanes to classify the data into two categories. It is based on the principle of structural risk minimization(Flake & Lawrence, 2002; Wang & Hu, 2005). Due to its good performance in small-sample prediction, it has gained attention in literature for ground vibration prediction (Hasanipanah et al., 2015; Khandelwal, 2010, 2011a, 2011b; Mohammadnejad et al., 2012). And suitability of different types of SVM were accessed (Temeng et al., 2022). In these studies, SVM was utilized to predict PPV, synthesizing the two parameters: distance between the monitoring point and blast point, and the maximum charge per delay.

In non-linear regression case, the vital hyperparameters of SVM are C, ε and γ. They have a significant effect on final prediction. Traditionally, grid search, as an exhaustive method, is utilized to determine the best hyperparameter of a model. The limitation of this approach is obvious, low efficiency. In this context, particle swarm optimization (PSO), an evolutionary optimization algorithm (H. Liu & Han, 2017; Zambrano-Bigiarini et al., 2013), is considered a candidate method for hyperparameter tuning in this study.

Literature gap and objectives of the study

Although the various predictors have been developed widely in the literature, it is still a challenging topic due to its multifaceted and critical nature, including the challenges of complicated relationships, the lack of large datasets, the various relative parameters, and the specificity of the mine conditions. So, the main purpose of this study is to build a universal and efficient predictor that can provide an

accurate prediction with a small dataset, which can assist the engineers to control the vibration.

Even though SVM has been developed by many researchers for PPV prediction in the existing literature, there is no paper combining PSO and RF with SVM. In this context, this paper established a novel model based on SVM for PPV prediction. In this model, RF is applied for feature selection and PSO is applied for hyperparameter tuning. The feasibility and superiority of this model are demonstrated by comparison with MLR and empirical models. These models are employed to conduct the prediction of PPV on a mine located in Istanbul. To assess the stability of the prediction, 10-fold cross-validation is applied in the training process of every model.

The collected dataset is explained in section 2. In section 3, a basic methodology of SVM, PSO, RF and other related techniques are introduced. In section 4, the code metadata is illustrated. Then in section 5, the effectiveness of PSO on SVM is demonstrated. The accuracy of PSO-SVM, MLR and empirical models are listed and discussed. The influence caused by different input dimensions and the validity of RF in feature selection are investigated as well. The novelty and superiority are illustrated in section 6. Finally, the limitation and potential future scope is provided in section 7.

Field investigation

The dataset utilized in this study was collected at Akdaglar Quarry of Cendere basin in northern Istanbul. The mine is very close to the urban area (as shown in AppendixB). The blast data is collected by seismographs inserted in 88 blasting monitoring points.

In this dataset, the measured indicator of ground vibration is PPV. The blasting design parameters are also recorded: bench height H, drilled burden B, spacing S, blasting hole diameter D, subdrilling U and stemming T. They are represented as a series of ratios: H/B, S/B, B/D, U/B and T/B.

Power factor PF, as a basic blast design parameter, is recorded. Besides, distance from the monitoring point d, maximum charge per delay Q and scaled distance Sd are collected as well. For convenience, these parameters are represented as: X1=S/B, X2=H/B, X3=B/D, X4=T/B, X5=U/B, X6=PF, X7=Q, X8=d, X9=Sd, Y1=PPV.

The distribution of each parameter is shown in the histograms in the diagonal of figure 2. Figure 2 is a scatter matrix of the dataset. In the scatters, every parameter is plotted with each other to observe the correlation. It is worth noting that Y_1 does not have obvious linear-like relationship with X parameters except $X_8(d)$, $X_9(Sd)$. This is because distance (d) has significant correlation with PPV.

As to $X_9(Sd)$, it does not only have apparent with PPV, but with X_8. This is because the scaled distance is obtained from X with the equation: $Sd = {}^{d}$, which means $X_9(Sd)$ should be isolated from X_8 and X_7 in feature selection.

The obvious relationship between X_9 and PPV may imply that maximum charge per delay $X_7(Q)$ also has a relationship with PPV besides $X_8(d)$. This is reasonable as Q and d have been widely utilized as one of inputs in existing blast-induced vibration predictors. Additionally, several blast design parameters such as X (^{B}) and X (^{T}) have effect on PPV according to the scatter. For quantized importance of each parameter, RF is employed. The importance of each feature calculated by RF is shown in figure 3.

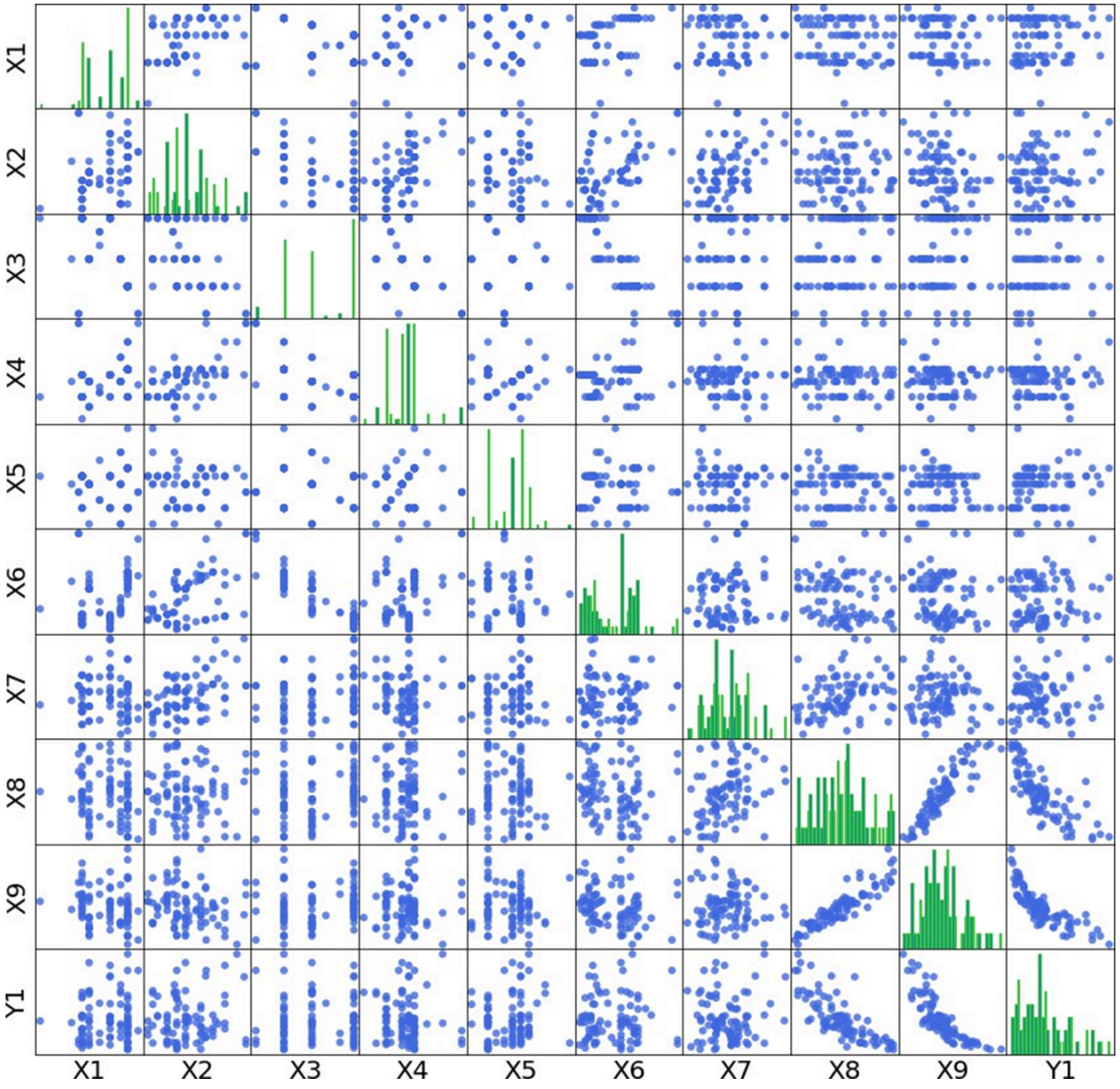

Figure 2 Scatter-matrix of the dataset

Methodology

Sample split and data pre-processing

To evaluate the ability of generalization of the models, the dataset can be split into a train set and a test set before developing the proposed techniques. One popular way to partition the dataset is to randomly or stratify the dataset into train set, validation set and test set. The model will finally be evaluated with the test set.

However, when the sample size of available datasets in the field of blast-induced ground vibration is limited, this method can waste data as the test dataset is isolated during the training process. To address this problem in a small sample dataset, K-Fold cross-validation, a resampling procedure, is applied to divide the dataset and evaluate the model. The only parameter of this method is the number K, referring to the total number of groups split from the original dataset. In each group, a number of n/k data is allocated as test data, with the remaining defined as train data. The final evaluation score (such as R-squared value R^2) will be the mean of the score attained from these k groups. The purpose of using K-fold cross-validation is to utilize all the data in the training process so that the whole data characteristics are represented and prevent the model from overfitting. In this paper, the K value is set as 10.

The outliers of the dataset are detected and replaced with the mean without it to reduce the influence of large data. The parameters in the dataset have a series of different physical units and varying values. In this condition, to transform them to a similar scale and improve data integrity, all the data were normalized with MinMaxScaler, the equation is:

$$x_{scaled} = \frac{x - x_{min}}{x_{mas} - x_{min}} \tag{1}$$

Model evaluation

To evaluate the accuracy of the proposed model, three statistic indices are used: R-squared (R^2), Mean Square Error (MSE) and Mean Absolute Error (MAE). The equations are as follows:

$$R^2 = 1 - \frac{\sum_{i=1}^{n}\left(y_{true_i} - y_{p_i}\right)^2}{\sum_{i=1}^{n}\left(y_{true_i} - \overline{y_{true}}\right)^2} \tag{2}$$

$$MSE = \frac{1}{n}\sum_{i=1}^{n}\left(y_{true_i} - y_{p_i}\right)^2 \tag{3}$$

$$MAE = \frac{1}{n}\sum_{i=1}^{n}\left|y_{true_i} - y_{p_i}\right|^2 \quad (4)$$

The results of each model are listed and analyzed in section 5.3.

Feature selection

As the input data is total 8 dimensions (exclude X_9, which is obtained from X_8 and X_7) and the contribution of each parameter to the prediction is unknown, the feature selection is essential for an accurate and generalized prediction.

Firstly, the importance of each feature is analyzed by a random forest (RF) algorithm. RF, an ensemble algorithm of decision tree predictors, measures the importance of each feature by observing how much the performance would drop if that feature is removed or rendered useless. For details of random forest, please refer to (Breiman, 2001). Figure 6(a) is the importance of each feature for illustrating the relative degree of each feature.

Support vector machine

Support vector machine (SVM) is a supervised machine learning model developed in AT&T Bell Laboratories (Cortes et al., 1995). It is originally inspired by binary classification questions. SVM aims to attain a separating hyperplane or a set of hyperplanes that maximize the distance to the nearest training data (margin). In this research, SVM is applied to a non-linear regression problem (so-called support vector regression, SVR). In the case of non-linear regression, SVR involves a set of non-linear transformations that can map the input vector into higher dimension space, so that the problem will also be mapped to linear regression in the higher dimension feature space. It is suggested that non-linear regression problems can be transformed to a quadratic optimization problem with SVR (Cherkassky & Ma, 2004; Flake & Lawrence, 2002; Hong et al., n.d.; Raj et al., 2019).

It can be expressed as: Find an estimator f:

$$f(x) = \sum_{i}^{M}\left(\alpha_i - \alpha_i^*\right)K\left(x_i, x\right) + b \quad (5)$$

where $K(x_i, x)$ is the kernel function, α_i and α^* are Lagrange multipliers.

That can:

$$min\frac{1}{2}||w||^2 + C\sum_{i=1}^{D}\left(\xi_i - \xi_i^*\right) \quad (6)$$

And it is subject to :

$$y_i - wx_i - b \leq \varepsilon + \xi_i \quad (7)$$

$$wx_i + b - y_i \leq \varepsilon + \xi_i^* \quad \text{where} \quad i = (1, 2, 3, \ldots, D) \quad (8)$$

$$\xi_i, \xi_i^* \geq 0 \quad (9)$$

where D is the dimension of the input vector, ξ_i and ξ^* are the slack variable penalizing the loss function, C is the positive regularization parameter determining the degree of the empirical error, and ε , as said above, is the margin of tolerance.

In this paper, Gaussian kernel function (or called radial basis function, RBF) is utilized as it has showed a good performance in non-linear regression (Lima et al., n.d.; Ma et al., 2018; Wang et al., n.d.). The Gaussian kernel function is:

$$K(x_i, x_j) = exp\left(-\frac{||x_i - x_j||^2}{2\sigma^2}\right) \quad (10)$$

Where σ is the variance and one of the hyperparameters, $||x_i - x_j||^2$ is the Euclidean distance between two points X_1 and X_2.There are three main hyperparameters that affect the performance of SVR a lot:

1. C, a trade-off parameter between prediction error and the flatness of the solution. If C is larger, the training error drop, but the ability of the generalization of the model decreases as the machine attempts to fit all the training data with a risk of overfit. Conversely, if C is smaller, the derivatives are small, but the accuracy of the prediction is influenced.
2. Similarly, ε, the margin of tolerance, determining the area that no penalty given to errors. A larger ε means a larger admitted error in training. As $\varepsilon \rightarrow 0_+$, every error is penalized.
3. $\gamma = \frac{1}{2\sigma^2}$ Is a hyperparameter when using RBF kernel function, defining how far training points reach the decision boundary. It is related to the degree of curvature of the decision boundary. A smaller γ leads to a Gaussian with a large variance implying that the support vector has a more wide-spread influence.

A well-trained SVR model should be balanced between accuracy and ability of generalization. Therefore, the tuning of these three hyperparameters is the key to training the model.

Particle swarm optimization

As discussed in section 3.4, there are three main hyperparameters affecting the performance a lot: C, ε and γ. Particle Swarm Optimization (PSO) has been widely developed in the optimization of hyperparameters when applying various ML techniques. In this paper, PSO, an evolutionary algorithm, where each iteration involves an update of a population of particles, which adapts by randomly returning to previously successful regions (Broderick & Howley, 2014; Shi & Eberhart, 1999).

The set of candidate solutions in the search space (the dimension of search space is the number of input parameters) are stored in terms of a particle in the swarm. Each particle has two attributes, position $x_{i,d}^{t}$ and velocity v_{i}^{t} in the search space, where $d = 0, 1,..., D$ refers to the d_{th} dimension of input variables (here, $D = 2$ as three hyperparameters are going to be optimized), $i = 0, 1,..., I$ denotes the i_{th} particle in the swarm (I for the population size), and $t = 0, 1,..., T$ represent the t_{th} iteration or generation in the PSO process. In the first generation, x^0 and v^0 (i =i,d i,d 0,1, … I, d = 0,1, … D) are randomly initialized. In the following iteration, the particles are updated taking the particle best position and population best position into account. The particle best position of the ith particle denotes as $P_{best}d$ (d = 0,1, … D), while the global best position $G_{best}d$ (d = 0,1, … D). They are updated in each new generation and based on fitness value (R2). The position and velocity of each particle is updated as:

$$v_{i,d}^{t+1} = w \times v_{i,d}^{t} + c_1 \times r_1^{t} \times \left(P_{best}{}_{i,d}^{t} - x_{i,d}^{t} \right) + c_2 \times r_2^{t} \times \left(G_{best}{}_{i,d}^{t} - x_{i,d}^{t} \right) \quad (12)$$

$$x_{i,d}^{t+1} = x_{i,d}^{t} + v_{i,d}^{t+1} \quad (13)$$

where i = 0,1, … I, d = 0,1, … D, t = 0,1, … T; w is the positive constant inertia weight coefficient, affecting the impact of velocity evolution on current velocity; c_1 and c_2 are constants so-called learning coefficients; r_1 and r_2 are uniformly distributed random values in range [0, 1].

RF-PSO-SVM model for vibration prediction

This paper developed an RF-PSO-SVM model to predict the blast-induced ground vibration, applying PSO to optimize three hyperparameters of SVM (C, ε and γ) and RF to select features. The parameters of the model are listed in table 1(b). The model used the sk-learn library to build and train the SVM and MLR model. The model also referred and modified the open-source code for the implements of PSO.

The main steps of the proposed model are shown in table 1(a).

TABLE 1a Main steps of RF-PSO-SVM

Steps number	Description
Step 1.	Load data from the file and conduct the pre-process.
Step 2.	Apply random forest to select feature.
Step 3	Initialize PSO: Randomly generate the first population. That is randomly set the velocity $v_{i,d}^0$ and position $x_{i,d}^0$ $(i = 0,1, \dots I,\ d = 0,1, \dots D)$ of each particle. The position vector denotes the solution set of C, ε and γ. Setup the parameters of PSO: I , D , T, w, c_1 and c_2.
Step 4.	Attain the initial particle best and population best position: for each particle set the current position as ${P_{best}}_i^0$ $(i = 0,1, \dots I)$ and the optimal individual position as the population best position ${G_{best}}^0$.
Step 5.	Evaluate the fitness value of each particle. The fitness value is the average R2 computed by 10-fold cross validation. It will increase the computing and time complexity but improve the stability of the fitness evaluation.
Step 6.	Update ${P_{best}}_i^t$ and ${G_{best}}^t$: for particle i, compare and the current position x_i^t with the ${P_{best}}_i^{t-1}$ according to fitness value evaluated in step 5 and update ${P_{best}}_i^t$. For the current population, choose the particle position with the maximized fitness value and compare it with previous global best position ${G_{best}}^{t-1}$ and update ${G_{best}}^t$
Step 7.	Check if it reaches the stopping criteria (i.e., reaching the maximum iteration number T): if not, go to next generation $(t = t + 1)$, update the velocities $v_{i,d}^t$ and $x_{i,d}^t$ $(i = 0,1, \dots I,\ d = 0,1, \dots D)$, then start again from step 4; if yes, return the global best position ${G_{best}}^t$ and end PSO process.
Step 8.	Return the best hyperparameter. Train the SVM model and attain accuracy indicators.
Step 9.	Decrease the input dimension by 1 according to importance histogram
Step 10.	Repeat the process from step 2 to decide the optimal input dimensions until the input dimension is two.
Step 11.	Attain the optimal feature dimension and the corresponding hyperparameters

TABLE 1b Parameters in PSO-SVM

	Type	Denotes	Interpolation
RF	Hyperparameter	Max_{dep}	Maximum depth of the tree ($Max_{dep} = 10$)
SVM	Hyperparameter	C	Regularization parameter
		ε	Margin of tolerance
		γ	Parameter when using RBF kernel function
PSO	Constants	I	The population size ($I = 50$)
		D	The number of the dimension of input vector ($D = 3$)
		T	The number of maximum iterations ($T = 60$)
		w	Inertia weight coefficient ($w = \frac{1}{2\ln 2}$)
		c_1	Learning rate ($c_1 = \frac{1}{2} + \ln 2$)
		c_2	Learning rate ($c_2 = \frac{1}{2} + \ln 2$)
	Fitness value	R^2	R-squared Fitness value
	Iterative vector	x_{id}^t	Position of ith particle in dth dimension in tth generation
		v_{id}^t	Velocity of ith particle in dth dimension in tth generation
		${P_{best}}_i^t$	The history best position of ith particle in tth generation
		${G_{best}}^t$	The history global optimal position in tth generation

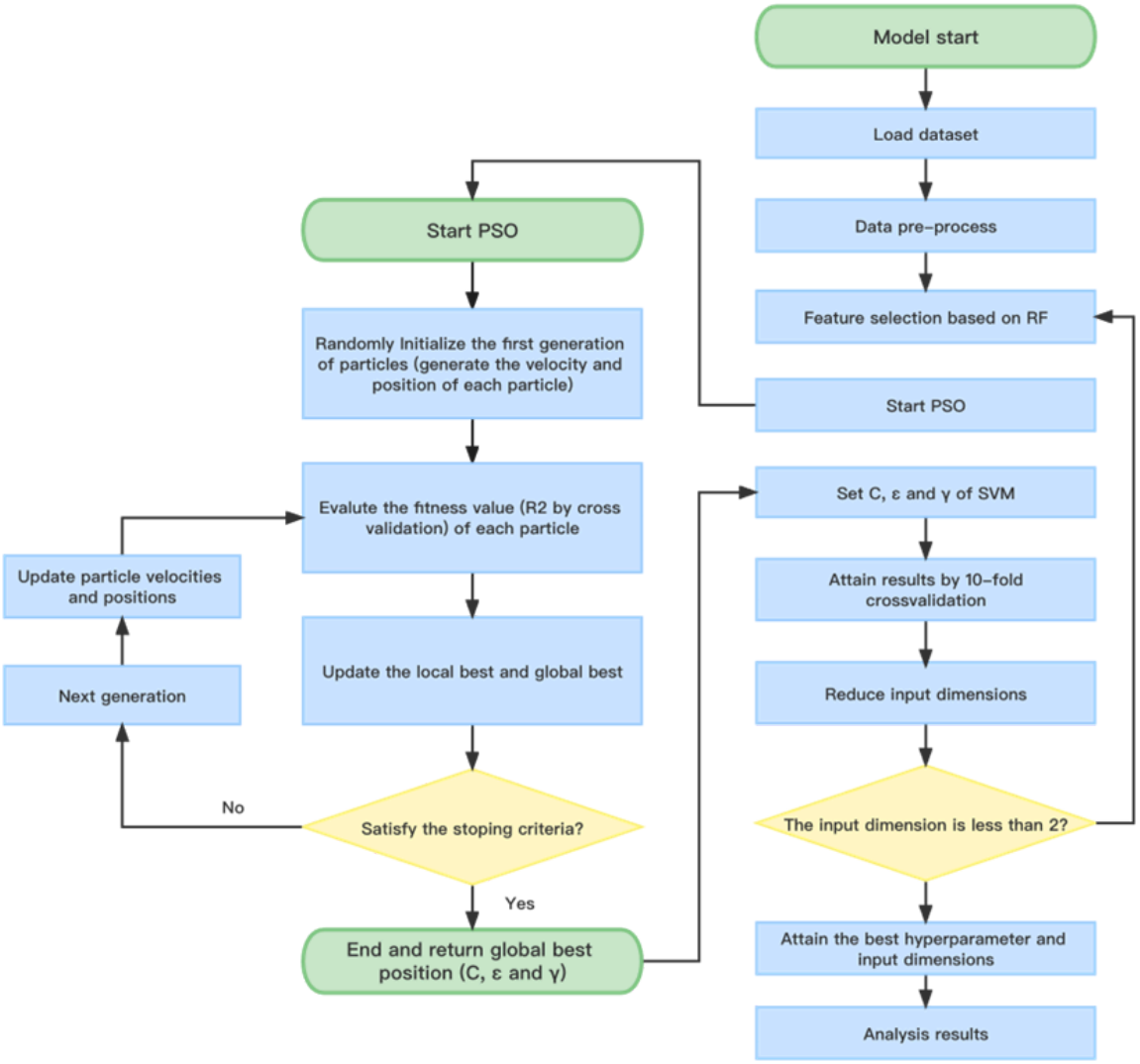

Figure 3 Flow chart of RF-PSO-SVM model

Figure 3 is the flow chart of the above main steps of RF-PSO-SVM.

Other existing methods for vibration prediction

Multivariate linear regression

Multivariate linear regression (MLR) is introduced to learn about the linear relationship between a series of independent variables or features and a dependent variable or target. It aims to generate a line for linear regression. To attain this line (i.e., fit the relationship linearly), the weights ($\beta = \beta_1, \beta_2, \beta_3, \ldots \beta_8$) of the input variables were calculated.

$$PPV = \beta_0 + \beta_1 X_1 + \beta_2 X_2 + \beta_3 X_3 + \cdots + \beta_8 X_8 + \epsilon \quad (14)$$

Where $\boldsymbol{X}$ = X_1, X_2, X_3, … X_8 represents the features of the dataset which are: correspondingly. β_0 is the y-intercept and ϵ is the error term of the model (so called residual).

Empirical models

The empirical models implemented in this paper are three most popular ones: Duvall and Petkof (USBM), Ambraseys–Hendron and Indian standard which are the most popular models in the literature. The equations are as follow:

USBM: $PPV = \alpha\left(\frac{D}{\sqrt{Q}}\right)^{\beta}$ (15)

Ambraseys-Hendron: $PPV = \alpha\left(\frac{D}{Q^{1/3}}\right)^{\beta}$ (16)

Indian standard: $PPV = \alpha\left(\frac{D}{Q^{2/3}}\right)^{\beta}$ (17)

Where D is the distance between monitoring point and the blast point, and Q is the maximum charge per delay. Provided with the form of the equation, the key is to find two constants involved in the equation. SPSS, a statistical analysis software, was used in this research.

Code Metadata

This project was built and implemented on Google Colab with Python (≥3.5) and the tools built in this study are packaged up in the GitHub repository.

The standard libraries used are listed as follows:

- Scikit-learn (≥1.1.1): for SVM and MLR building and training
- Matplotlib (≥3.4.3): for plotting and visualization.
- NumPy (≥1.22.3): for data processing.
- Pandas (≥1.4.1): for data processing. Besides, SPSS was used to build empirical models.

In the Colab notebook, the RF-PSO-SVM, MLR models are implemented. The analysis of accuracy, stability and convergence are implemented and run in the notebook with a clear content. All the outputs including relevant plots are already shown in the notebook.

Results

In this section, the proposed RF-PSO-SVM will be employed on the current dataset. To evaluate the feasibility and effectiveness of PSO, the important stages in the optimization process in PSO-SVM modelling is visualized in section 5.1. In section 5.2, the influence on prediction accuracy caused by various input dimensions is discussed, and the best choice of input dimension (in current dataset) is made for the following analyses. For indicating the capability of proposed RF-PSO-SVM, it is compared with the popular predictive approaches existing in the literature: MLR and three empirical models. The corresponding R^2, MSE and MAE are computed and compared in section 5.3. The stability of prediction is discussed in section 5.4

Convergence of PSO-SVM

In this section, it is preliminary to optimize the hyperparameter by PSO with input of 9 dimensions. However, the different input dimensions can influence the predict, which is discussed in section 5.2.

As shown in figure 5, the fitness value converges after around 13 iterations with the best fitness value R^2 = 0.72948 in best position. Figure 4 shows the distribution of particles at iteration 0, 10 ,20 and the final iteration. In the first iteration, there are randomly set particles, distributed randomly in the search space preventing the evolution from moving towards in only one direction. At this moment, the fitness value varies from 0.1 to 0.6 approximately. In iteration 10, the particles gathered with the

$G_{best}{}^{10}$ improved from 0.6 to 0.7 approximately. There are some particles with satisfying fitness values away from the gathering to explore more potential solutions. Then in iteration 20, fig shows that the best fitness value begins to converge, but there are still some particles exploring outside the 'optimal' group to remain the possibility of other possible solutions. Finally, they become closer than ever with fitness value R^2 ranging from 0.727 to 0.729 approximately. The total computing time is 172s.

Grid search was conducted as well. The range of the three hyperparameters keeps the same as PSO. But the increment of each hyperparameter is 20, because when the step was lower than 20, the grid search process took more than one hour to compute. The fitness value R^2 obtained with the optimized hyperparameters is 0.715 with a computing time of 240s approximately. This result indicates that PSO is more efficient than grid search in hyperparameter tuning.

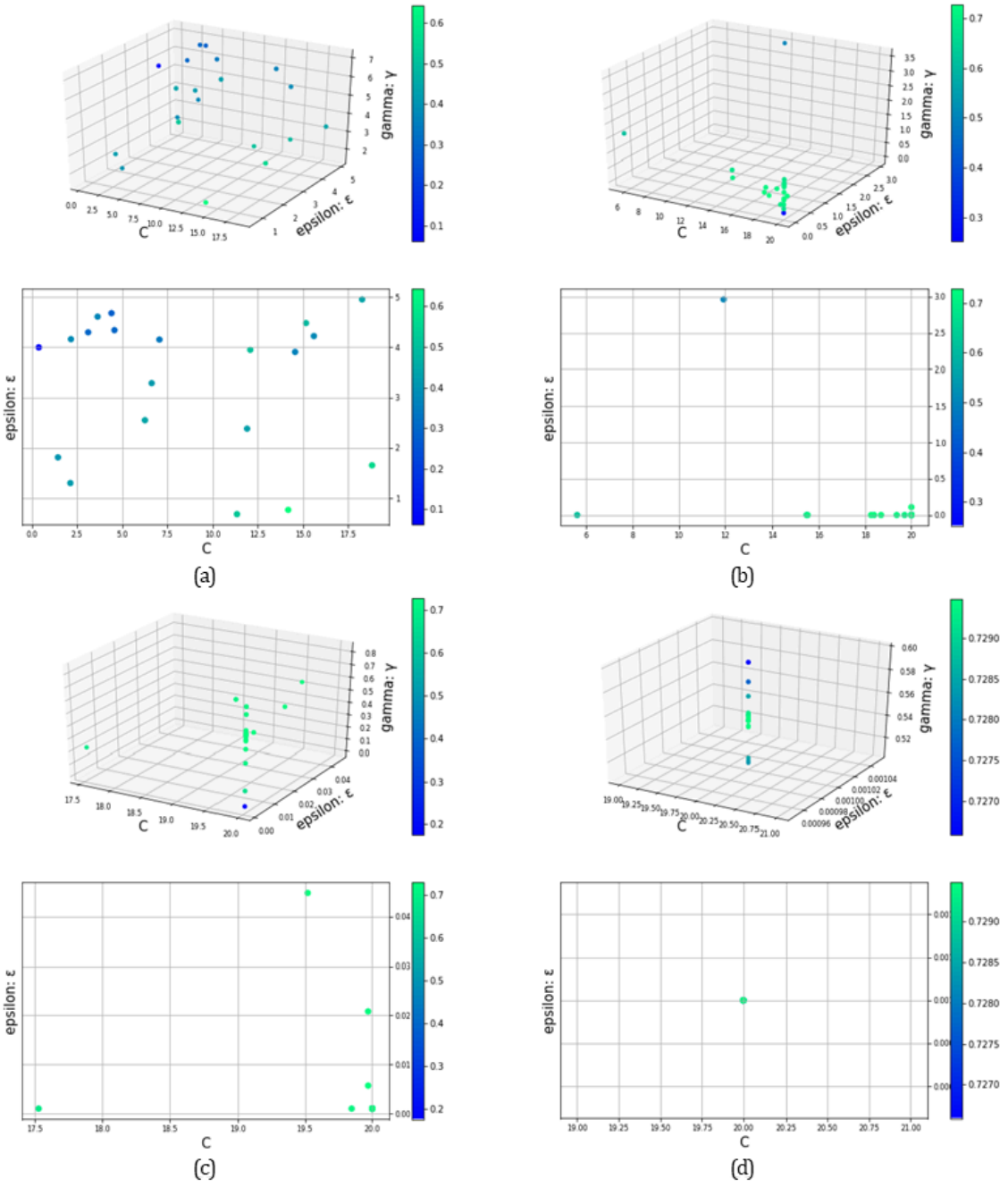

Figure 4 Particle distribution of 0 iteration (a), 10th iteration (b), 20th iteration (c), and the final iteration (d)

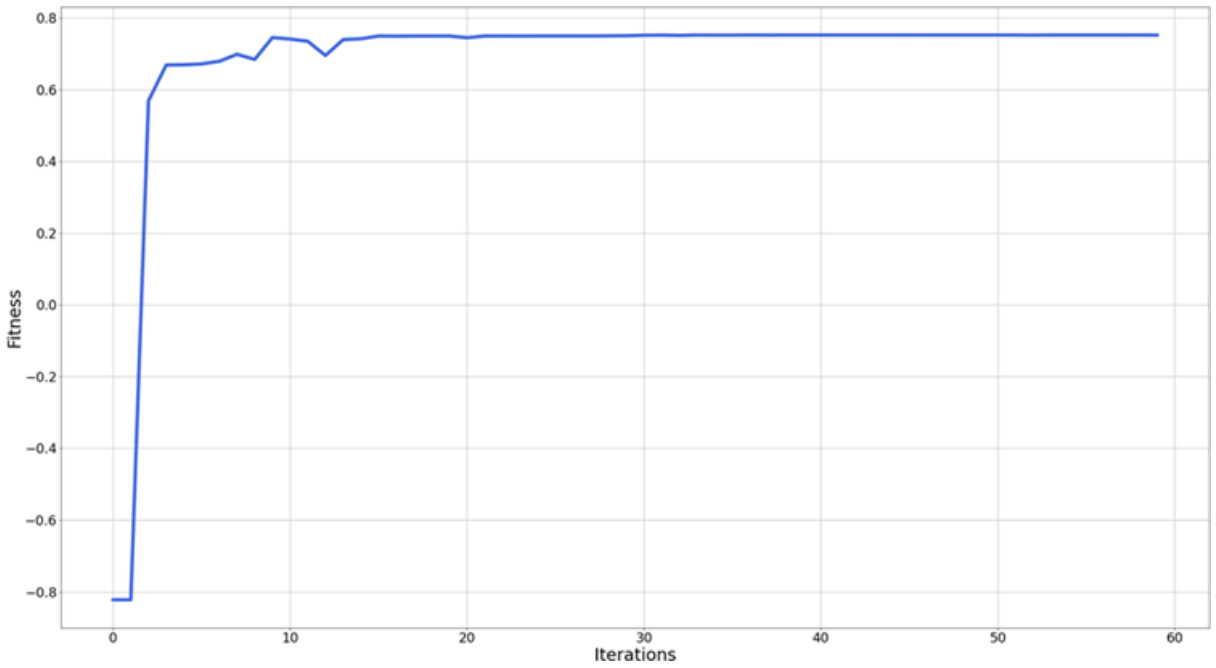

Figure 5 Convergence plot

PSO-SVM with different input dimensions

In this dataset, there are a total 9 dimensions in the feature space. As discussed in the field investigation section, there are 8 valuable features to select. The feature selection is an important process. If the input dimension is small such as 2, the model might be not capable of fetching all the relationships between input and output. Inversely, the model may fall into overfitting.

To observe the influence of different input dimensions caused to final model prediction accuracy, 8 different groups of inputs are applied to predict PPV. The dimension of feature space in each group decreases according to the importance indices produced by RF shown in figure 6(a). Illustratively, the inputs are all these features in the first group, top 7 features are set as the inputs in the second group, top 6 features are utilized in the third group, and so on. In the last group, only X_8 are used for prediction. The SVM models in every group are trained and validated with cross-validation, the optimal hyperparameters of the SVM models are attained by PSO.

As shown in figure6 (b), the elbow point occurs in the group with 5-dimension inputs. After that point, the accuracy drops slightly as the dimension increases and is always higher than 0.73 until group 8, which may imply that the model is overfitted with higher dimensions, especially with 8 inputs. Another reason is that X_3 feature may have produced noise, in other words, X_3 negatively influence the prediction performance.

Before that point, the model is still able to predict an acceptable predicted result until dimension of 1. This may because, X_8 is not sufficient to contribute to build a model to predict PPV with itself even though it has a significant importance shown in figure 6(a). The best result is witnessed in the group with 5 dimensions X2, X5, X6, X7 and X8 with an R^2 of 0.7716. So, the model trained by 5-dimension input was selected to compare the performance of other existing methods afterwards (MLR and empirical models).

According to the result, the future data collection may focus on recording the top features X2, X5, X6, X7 and X8 to reduce the cost of field investigation.

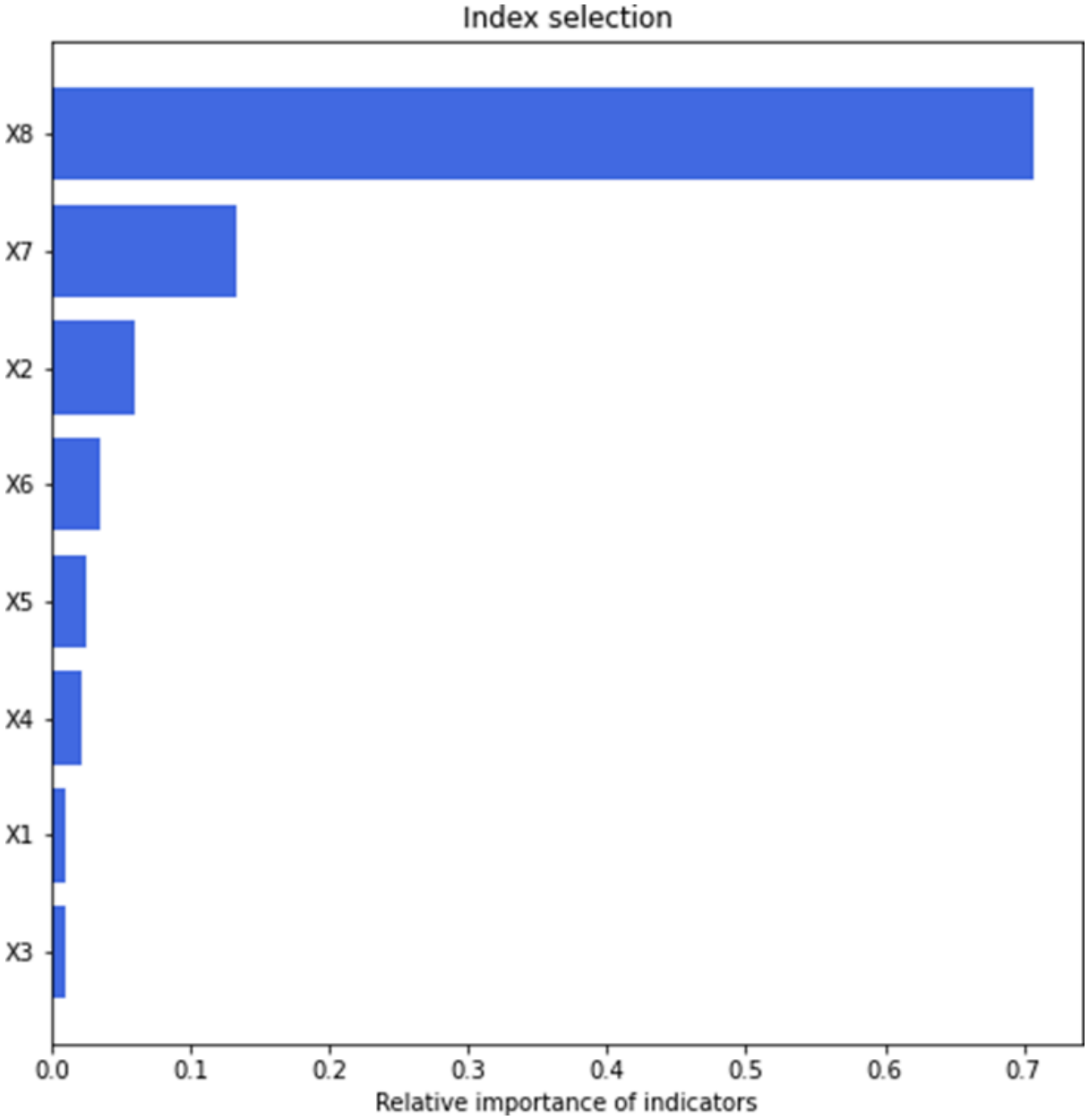

Figure 6a Importance histogram

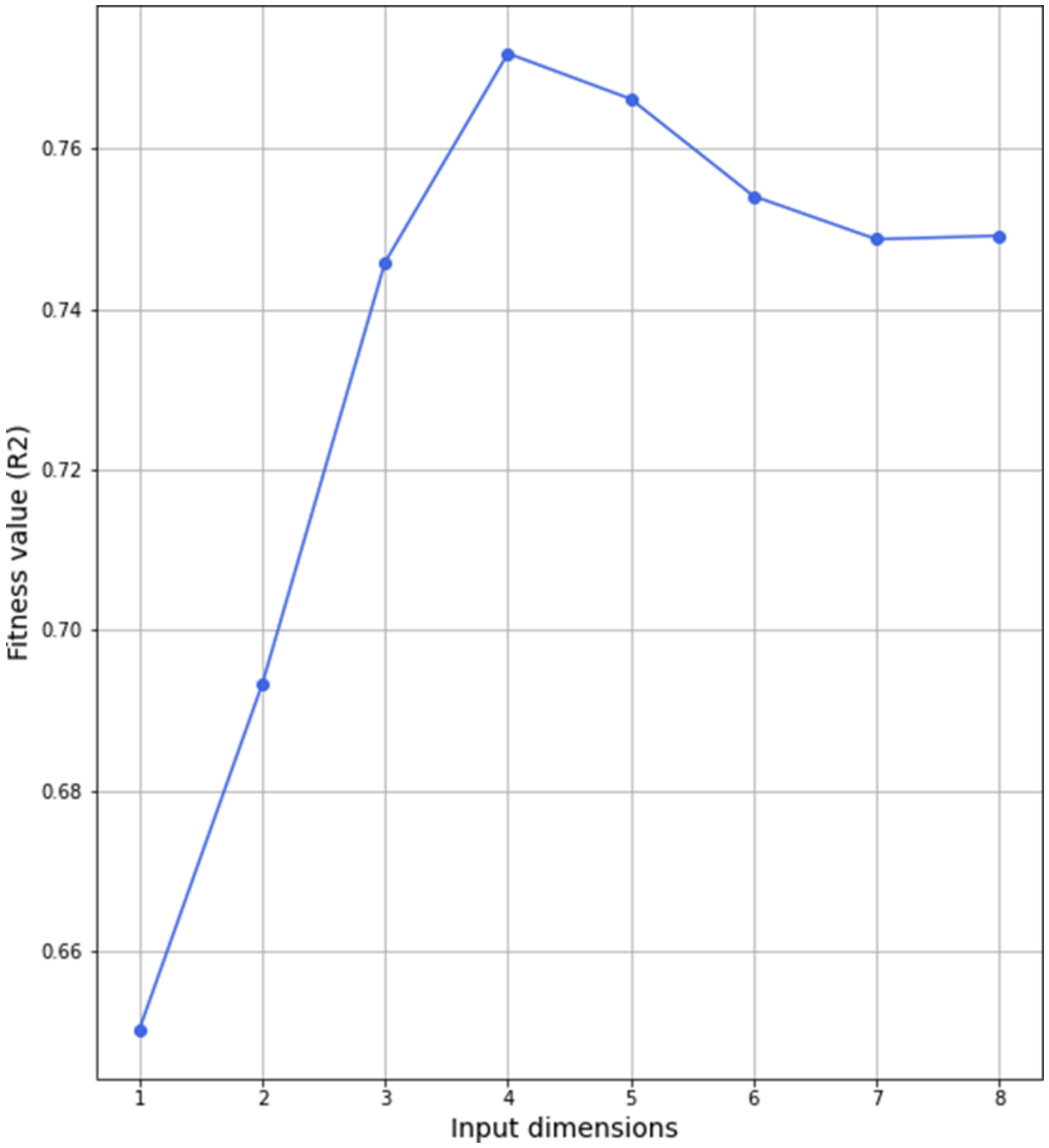

Figure 6b Variance plot

Prediction accuracy analysis

In this section, the performances indices (R^2, MSE, MAE) of PSO-SVM are listed and compared with that of MLR and empirical models.

Figure 7 shows the plots measured value vs predicted value of the proposed PSO-SVM (figure7 (a)), MLR (figure7 (b)) and empirical models (figure 7 (c) (d) (e)). The more points distribute around the line y = x, the more accurate the prediction is.

Note that 10-fold cross-validation is applied to every model, so there are 10 colors of points indicating 10 different validation-sets in the plot.

TABLE 2 Results of the model

	R^2	MSE	MAE
PSO-SVM	**0.7716**	**13.5979**	**2.7550**
MLR	0.6529	19.0265	3.4876
USBM	0.7111	18.1047	3.3685
Ambraseys–Hendron	0.7052	18.4659	3.3181
Indian standard	0.4634	33.6214	4.5793

R^2 value explains the percentage of the accuracy. The closer to 1 R^2 is, the predictive model is considered an excellent model. By contrast, R^2 approaching to zero always indicates that the prediction is not acceptable. As shown in table, PSO- SVM has the best R^2 score of 0.7716 representing that PSO-SVM provides a substantial prediction. It is 18.18% higher than MLR and 8.51% higher than USBM which is the empirical model with the highest R^2 in the three approaches. It is worth noting that there is one model that has a R^2 value smaller than 0.5, meaning that the model has a weak effect.

In terms of MSE, it is acting as an error indicator whose value represents the degree of the prediction deviating from the measured (true) data. As it is a squared value, the errors will be amplified. A model with a MSE value close to zero means it is an accurate predictor. In the table, PSO-SVM shows the lowest value of 13.5979, 28.53% lower than MLR and 24.89% lower than USBM.

However, MSE is easy to be affected by outliers, so MAE is calculated as well. MAE is a row level error indicator that takes the absolute value of error into account. It has shown a good robustness ability when facing outliers. Similar to MSE, the smaller MAE is, the better agreement with measured data the prediction is made.

PSO-SVM still has the lowest in MAE indicated (2.7550), 21.01% lower than MLR and 16.9% lower than Ambraseys–Hendron (the empirical model with lowest MAE). It is also worth noting that, the benchmark MLR show a poor performance with R^2 less than 0.7, this may imply that there is not a significant linear relationship between the input data and output data.

The results above reveal that the RF-PSO-SVM is sufficient to provide a comparatively accurate prediction compared to MLR and the three empirical models.

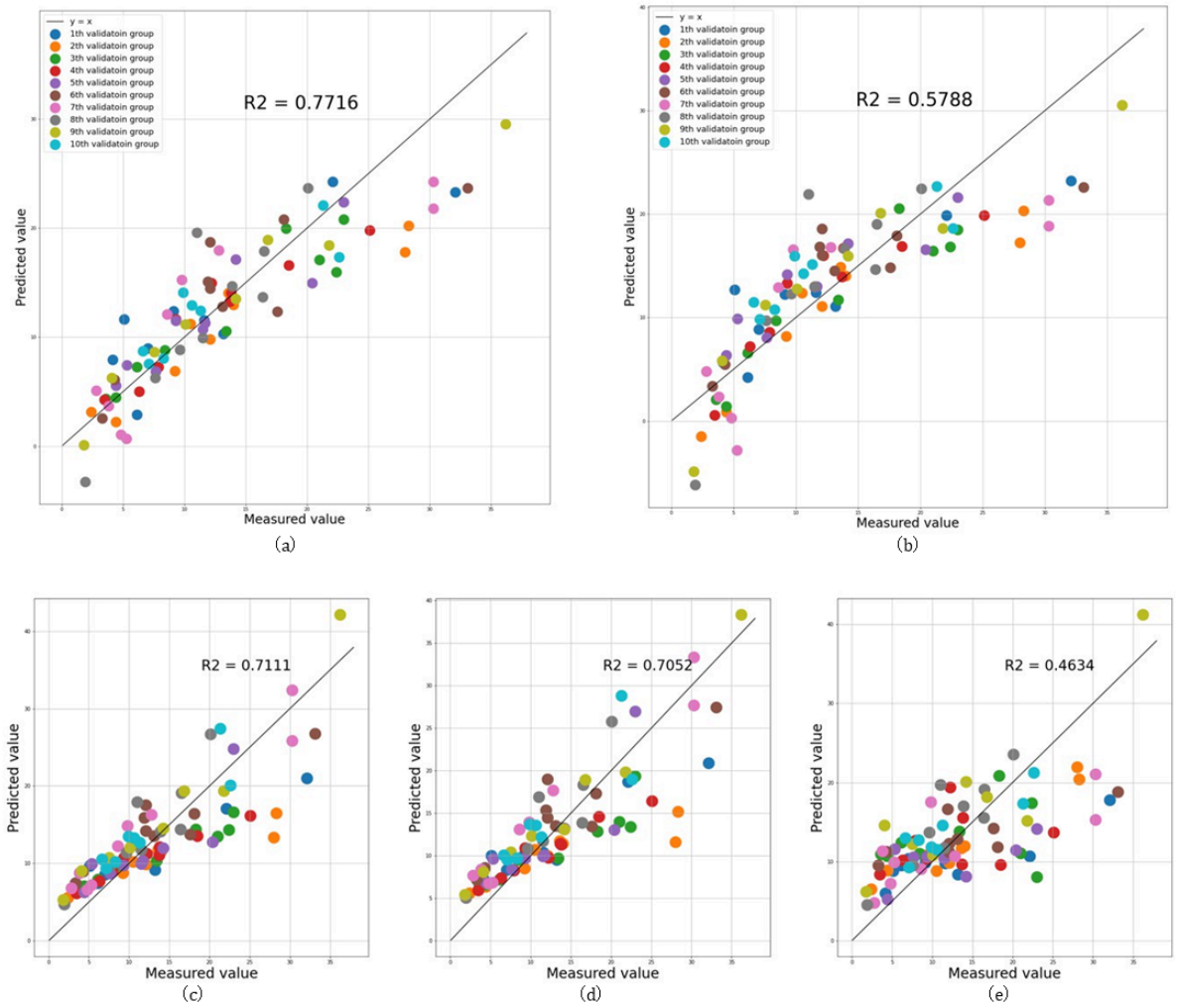

Figure 7 Predicted value vs. Measured value of model: PSO-SVM (a), MLR (b), USBM (c), Ambraseys-Hendron (d), and Indian standard (e)

Prediction stability analysis

Figure 8 is the variance of the evaluation indices (R^2, MSE, MAE) of the models. A plot close to a straight line means that the prediction is stable, and the variance of prediction is acceptable.

From figure8 (a) and figure8 (b) (plotting the variance of R^2 and MSE), it is obvious that PSO-SVM has relatively slight fluctuation compared to other models, indicating that PSO-SVM is the approach with the most stable performance. In terms of MAE, the difference between PSO-SVM and the others are not significant, this is because the MAE is an absolute value which is not a squared value as MSE does.

It is worth noting that the empirical models show a dramatic variance in terms of R^2 and MSE. This result illustrates that empirical models, which are established according to engineering experience, are not stable and generalized. In detail,

although in table, USBM and Ambraseys–Hendron have a satisfying prediction performance in the current dataset, they may not be suitable for other mines. The empirical model Indian standard is poor in this mine, but the accuracy may be improved when employed in other mines. This is because the empirical models are established with site-specific parameters such as rock density, rock type, etc. collected by rigorous field measurement.

PSO-SVM shows superiority in terms of the ability of generalization. It does require engineers to insert seismographs to measure data, but it does not rely on site-specific constants. It only takes a series of controllable parameters X2, X5, X6, X7 and X8 to fit the complicated relationship and provide an excellent prediction.

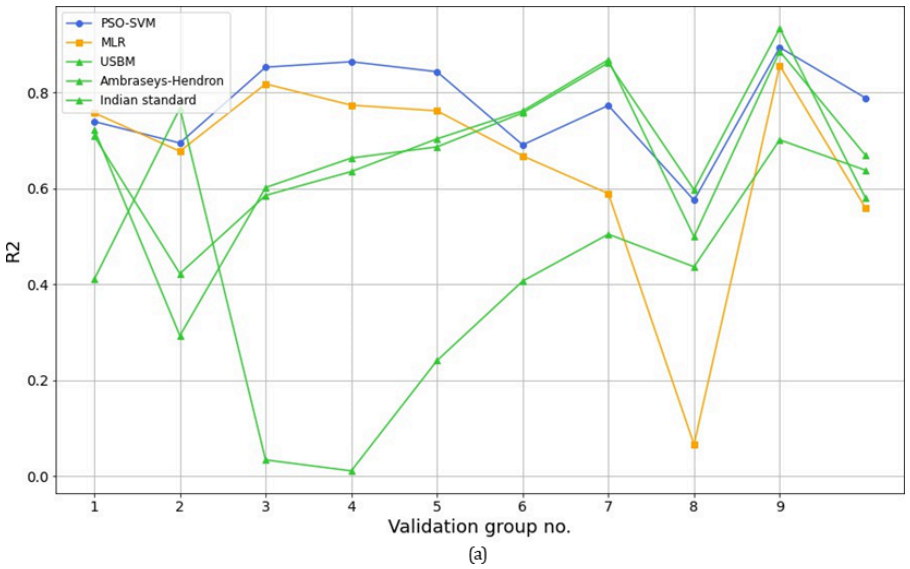

(a)

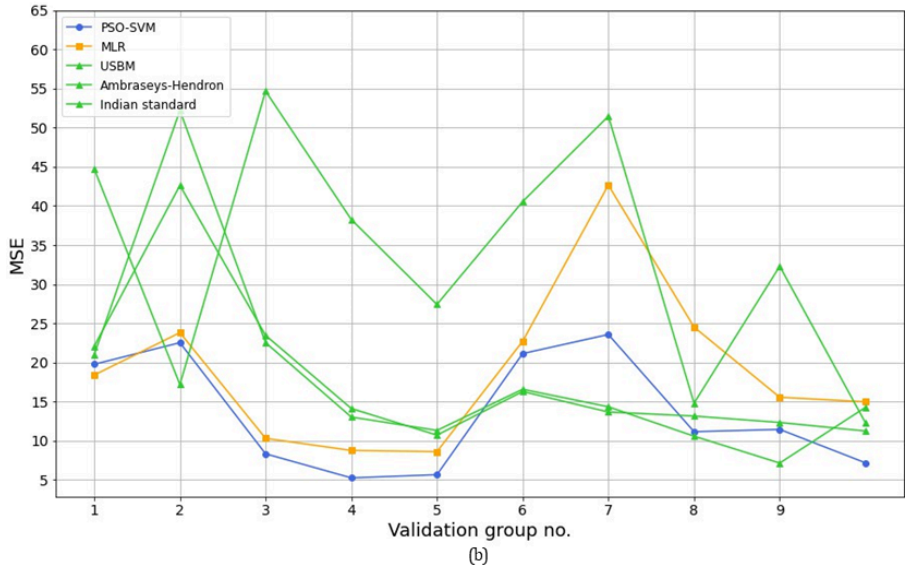

(b)

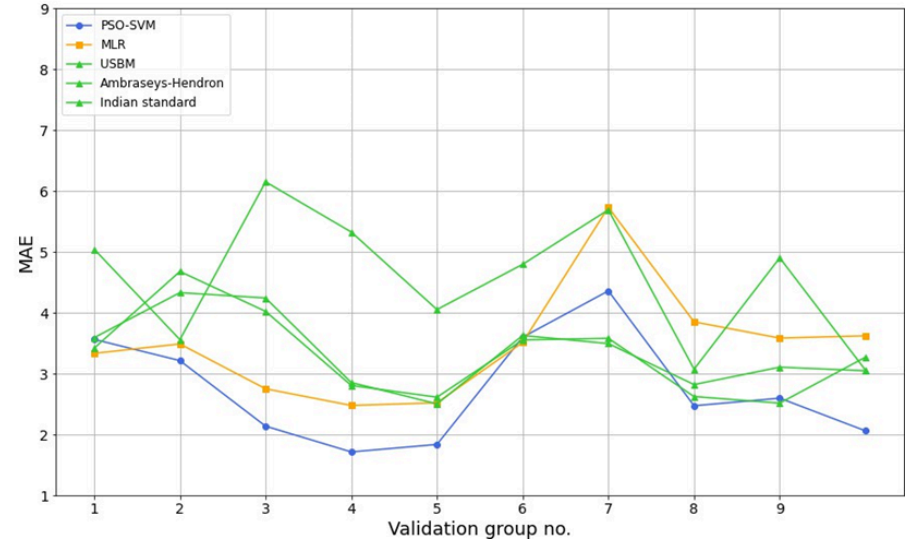

Figure 8 Variance plot for: R2 (a), MSE (b), MAE(c)

Conclusion

This paper proposed a novel model for particle peak velocity PPV (an indicator representing blast-induced ground vibration) prediction. The proposed model based on support vector machine algorithm (SVM). It also applied random forest (RF) to select features and used particle swarm optimization (PSO) for hyperparameter tuning (so this model is called RF-PSO-SVM). For purpose of comparison, MLR and three popular empirical models are implemented as well. The dataset is based on a mine located in Istanbul. In this dataset, there are 88 observation points. Several blast design parameters, distance and maximum charge per delay are recorded. To utilize all the data into usage, 10-fold cross-validation is employed in all models. The three models are evaluated with statistical indicators (R^2, MSE and MAE). Firstly, the analysis of astringency of PSO-SVM shows that PSO can keep activity in search space and converge efficiently to the optimal solution of hyperparameters. Then the variance plot of prediction accuracy caused by different input dimensions indicates that PSO-SVM has the optimal performance with R^2 of 0.7717 when the input is 5-dimension X2, X5, X6, X7 and X8 in the current dataset. The accuracy analysis reveals that PSO-SVM has the optimal accurate prediction with R^2 of 0.7717, MSE of 13.5979, and MAE of 2.755 compared to MLR and three empirical models. The stability result preliminarily shows that RF-PSO-SVM is capable of providing a stable and generalized prediction. According to the results, it is reasonable to conclude that the RF-PSO-SVM model has shown its superiority in blast-induced ground vibration prediction with its excellent capability for regression problem and satisfying ability of generalization, when the dataset is small. With the prediction conducted by the proposed model, the decision-makers can efficiently modify the blast design parameters to control the vibration.

Limitation and future scope

The main limitation of the study is the models are trained and tested with a single dataset. For a rigorous assessment of universal ability, a dataset of mines of various types and locations should be utilized.

Besides, more types of SVM such as least square support vector machine, relevance vector machine should be implemented and discussed as the performance of them varies on different datasets.

Moreover, this study only implemented random forest as the feature selection method. Different feature selection methods such as shape analysis could be implemented and discussed in the future work. In addition, some data mining methods for data augment can be a potential future scope. With a dataset of a large sample size, the performance and ability of generalization may be enhanced.

Acknowledgements

The author would like to acknowledge the support from the supervisors and acknowledge the support from Beyond Mining company.

References

[1] Ak, H., Iphar, M., Yavuz, M., & Konuk, A. (2009). Evaluation of ground vibration effect of blasting operations in a magnesite mine. Soil Dyn Earthq Eng, 29(4), 669–676. https://doi.org/10.1016/j.soildyn.2008.07.003

[2] Amiri, M., Bakhshandeh Amnieh, H., Hasanipanah, M., & Mohammad Khanli, L. (2016). A new combination of artificial neural network and K- nearest neighbors models to predict blast-induced ground vibration and air-overpressure. Engineering with Computers, 32(4), 631–644. https://doi.org/10.1007/S00366-016-0442-5

[3] Armaghani, D. J., Hasanipanah, M., Amnieh, H. B., & Mohamad, E. T. (2018). Feasibility of ICA in approximating ground vibration resulting from mine blasting. Neural Computing and Applications, 29(9), 457–465. https://doi.org/10.1007/S00521-016-2577-0

[4] Athanasopoulos, G. A., & Pelekis, P. C. (2000). Ground vibrations from sheetpile driving in urban environment: Measurements, analysis and effects on buildings and occupants. Soil Dynamics and Earthquake Engineering, 19(5), 371–387. https://doi.org/10.1016/S0267-7261(00)00008-7

[5] Bisoyi, S. K., & Pal, B. K. (2020). Prediction of Ground Vibration Using Various Regression Analysis. Journal of Mining Science 2020 56:3, 56(3), 378–387. https://doi.org/10.1134/S1062739120036665

[6] Breiman, L. (2001). Random Forests. Machine Learning 2001 45:1, 45(1), 5–32. https://doi.org/10.1023/A:1010933404324

[7] Broderick, I., & Howley, E. (2014). Particle Swarm Optimisation with Enhanced Memory Particles. Lecture Notes in Computer Science (Including Subseries Lecture Notes in Artificial Intelligence and Lecture Notes in Bioinformatics), 8667, 254–261. https://doi.org/10.1007/978-3- 319-09952-1_24

[8] Cherkassky, V., & Ma, Y. (2004). Practical selection of SVM parameters and noise estimation for SVM regression. Neural Networks, 17(1), 113–126. https://doi.org/10.1016/S0893-6080(03)00169-2

[9] Cherkassky, V., networks, Y. M.-N., & 2004, undefined. (n.d.). Practical selection of SVM parameters and noise estimation for SVM regression. Elsevier. Retrieved August 22, 2022, from https://www.sciencedirect.com/science/article/pii/S0893608003001692

[10] Cortes, C., Vapnik, V., & Saitta, L. (1995). Support-vector networks. Machine Learning 1995 20:3, 20(3), 273–297. https://doi.org/10.1007/BF00994018

[11] Deng, X., Zhu, J., Chen, S., Zhao, Z., … Y. Z.-… and U. S., & 2014, undefined. (n.d.). Numerical study on tunnel damage subject to blast-induced shock wave in jointed rock masses. Elsevier. Retrieved August 28, 2022, from https://www.sciencedirect.com/science/article/pii/S0886779814000534

[12] Dumakor-Dupey, N. K., Arya, S., & Jha, A. (2021). Advances in blast- induced impact prediction—a review of machine learning applications. Minerals, 11(6). https://doi.org/10.3390/min11060601

[13] Flake, G. W., & Lawrence, S. (2002). Efficient SVM regression training with SMO. Machine Learning, 46(1–3), 271–290. https://doi.org/10.1023/A:1012474916001

[14] Ghosh, A., & Daemen, J. J. K. (1983). A Simple New Blast Vibration Predictor (Based On Wave Propagation Laws). OnePetro.

[15] Gorai, A. K., Himanshu, V. K., & Santi, C. (2021). Development of ANN-Based Universal Predictor for Prediction of Blast-Induced Vibration Indicators and its Performance Comparison with Existing Empirical Models. Mining, Metallurgy and Exploration, 38(5), 2021–2036. https://doi.org/10.1007/s42461-021-00449-0

[16] Hasanipanah, M., Faradonbeh, R. S., Amnieh, H. B., Armaghani, D. J., Roohollah, ·, Faradonbeh, S., Hassan, ·, Amnieh, B., Danial, ·, Armaghani, J., & Monjezi, · Masoud. (2017). Forecasting blast-induced ground vibration developing a CART model. Springer, 33(2), 307–316. https://doi.org/10.1007/s00366-016-0475-9

[17] Hasanipanah, M., Monjezi, M., Shahnazar, A., Jahed Armaghani, D., & Farazmand, A. (2015). Feasibility of indirect determination of blast induced ground vibration based on support vector machine. Measurement: Journal of the International Measurement Confederation, 75, 289–297. https://doi.org/10.1016/J.MEASUREMENT.2015.07.019

[18] Hong, D., Systems, C. H.-I. T. on F., & 2005, undefined. (n.d.). Interval regression analysis using quadratic loss support vector machine. Ieeexplore.Ieee.Org. Retrieved August 22, 2022, from https://ieeexplore.ieee.org/abstract/document/1411825

[19] Hudaverdi, T. (2012). Application of multivariate analysis for prediction of blast-induced ground vibrations. Soil Dynamics and Earthquake Engineering, 43, 300–308. https://doi.org/10.1016/j.soildyn.2012.08.002

[20] Kabwe, E., Wang, Y., Kabwe, E., & Wang, Y. (2015). Airblast and Ground Vibration Monitoring at Chimiwungo Pit. Geomaterials, 6(1), 28–

38. https://doi.org/10.4236/GM.2016.61003

[21] Khandelwal, M. (2010). Evaluation and prediction of blast-induced ground vibration using support vector machine. International Journal of Rock Mechanics and Mining Sciences, 47(3), 509–516. https://doi.org/10.1016/J.IJRMMS.2010.01.007

[22] Khandelwal, M. (2011a). Blast-induced ground vibration prediction using support vector machine. Engineering with Computers, 27(3), 193–

200. https://doi.org/10.1007/S00366-010-0190-X

[23] Khandelwal, M. (2011b). Blast-induced ground vibration prediction using support vector machine. Engineering with Computers, 27(3), 193–200. https://doi.org/10.1007/S00366-010-0190-X

[24] Khandelwal, M., Kumar, D. L., & Yellishetty, M. (2009). Application of soft computing to predict blast-induced ground vibration. Engineering with Computers 2009 27:2, 27(2), 117–125. https://doi.org/10.1007/S00366- 009-0157-Y

[25] Khandelwal, M., & Singh, T. N. (2006). Prediction of blast induced ground vibrations and frequency in opencast mine: A neural network approach. Journal of Sound and Vibration, 289(4–5), 711–725. https://doi.org/10.1016/j.jsv.2005.02.044

[26] Kumar, R., Choudhury, D., and, K. B.-J. of R. M., & 2016, undefined. (n.d.). Determination of blast-induced ground vibration equations for rocks using mechanical and geological properties. Elsevier. Retrieved August 28, 2022, from https://www.sciencedirect.com/science/article/pii/S167477551600024X

[27] Kuzu, C. (2008). The importance of site-specific characters in prediction models for blast-induced ground vibrations. Soil Dynamics and Earthquake Engineering, 28(5), 405–414. https://doi.org/10.1016/J.SOILDYN.2007.06.013

[28] Larson, D. B. (1979). Spherical wave propagation in elastic media and its application to energy coupling for tamped and decoupled explosions. https://doi.org/10.2172/6256631

[29] Lima, A., Cannon, A., Geosciences, W. H.-C. &, & 2013, undefined. (n.d.). Nonlinear regression in environmental sciences by support vector machines combined with evolutionary strategy. Elsevier. Retrieved August 22, 2022, from https://www.sciencedirect.com/science/article/pii/S0098300412002269

[30] Liu, E. L., He, S., Xue, X., & Xu, J. (2011). Dynamic properties of intact rock samples subjected to cyclic loading under confining pressure conditions. Rock Mechanics and Rock Engineering, 44(5), 629–634. https://doi.org/10.1007/S00603-011-0151-8

[31] Liu, H., & Han, F. (2017). A modified standard PSO-2011 with robust search ability. Communications in Computer and Information Science, 791, 207–222. https://doi.org/10.1007/978-981-10-7179-9_16

[32] Ma, Z., Zhong, H., Xie, L., Xia, Q., & Kang, C. (2018). Month ahead average daily electricity price profile forecasting based on a hybrid nonlinear regression and SVM model: an ERCOT case study. Journal of Modern Power Systems and Clean Energy, 6(2), 281–291. https://doi.org/10.1007/S40565-018-0395-3

[33] Mohammadnejad, M., Gholami, R., Ramezanzadeh, A., & Jalali, M. E. (2012). Prediction of blast-induced vibrations in limestone quarries using support vector machine. Journals.Sagepub.Com, 18(9), 1322–1329. https://doi.org/10.1177/1077546311421052

[34] Monjezi, M., Singh, T. N., Khandelwal, M., Sinha, S., Singh, V., & Hosseini, I. (2016). Prediction and Analysis of Blast Parameters Using Artificial Neural Network: Http://Dx.Doi.Org/10.1260/095745606777630323, 37(5), 8–16

[35] Nateghi, R. (2011). Prediction of ground vibration level induced by blasting at different rock units. International Journal of Rock Mechanics and Mining Sciences, 48(6), 899–908. https://doi.org/10.1016/j.ijrmms.2011.04.014

[36] Navarro Torres, V. F., Silveira, L. G. C., Lopes, P. F. T., & de Lima, H. M. (2018). Assessing and controlling of bench blasting-induced vibrations to minimize impacts to a neighboring community. Journal of Cleaner Production, 187, 514–524. https://doi.org/10.1016/j.jclepro.2018.03.210

[37] Raj, J., (JSCP), J. A.-J. of S. C. P., & 2019, undefined. (2019).

Recurrent neural networks and nonlinear prediction in support vector machines. Irojournals.Com. https://doi.org/10.36548/jscp.2019.1.004

[38] Saadat, M., Khandelwal, M., & Monjezi, M. (2014). An ANN-based approach to predict blast-induced ground vibration of Gol-E-Gohar iron ore mine, Iran. Journal of Rock Mechanics and Geotechnical Engineering, 6(1), 67–76. https://doi.org/10.1016/j.jrmge.2013.11.001

[39] Shi, Y., & Eberhart, R. C. (1999). Empirical study of particle swarm optimization. Proceedings of the 1999 Congress on Evolutionary Computation, CEC 1999, 3, 1945–1950. https://doi.org/10.1109/CEC.1999.785511

[40] Singh, T., Kanchan, R., Saigal, K., & Verma, A. (2004). Prediction of p-wave velocity and anisotropic property of rock using artificial neural network technique. http://nopr.niscair.res.in/handle/123456789/5399

[41] Temeng, V. A., Arthur, C. K., & Ziggah, Y. Y. (2022). Suitability assessment of different vector machine regression techniques for blast- induced ground vibration prediction in Ghana. Modeling Earth Systems and Environment, 8(1), 897–909. https://doi.org/10.1007/s40808-021-01129-0

[42] Wang, H., brain, D. H. on neural networks and, & 2005, undefined. (n.d.). Comparison of SVM and LS-SVM for regression. Ieeexplore.Ieee.Org. Retrieved August 22, 2022, from https://ieeexplore.ieee.org/abstract/document/1614615

[43] Wang, H., & Hu, D. (2005). Comparison of SVM and LS-SVM for regression. Proceedings of 2005 International Conference on Neural Networks and Brain Proceedings, ICNNB'05, 1, 279–283. https://doi.org/10.1109/ICNNB.2005.1614615

[44] Zambrano-Bigiarini, M., Clerc, M., & Rojas, R. (2013). Standard Particle Swarm Optimisation 2011 at CEC-2013: A baseline for future PSO improvements. 2013 IEEE Congress on Evolutionary Computation, CEC 2013, 2337–2344. https://doi.org/10.1109/CEC.2013.6557848